High resolution on-chip optical filter array based on double subwavelength grating reflectors

Yu Horie,[1] Amir Arbabi,[1] Seunghoon Han,[1,2] and Andrei Faraon[1,*]

[1]*T. J. Watson Laboratory of Applied Physics, California Institute of Technology, 1200 E California Blvd, Pasadena, CA 91125, USA*

[2]*Samsung Advanced Institute of Technology, Samsung Electronics, Samsung-ro 130, Suwon-si, Gyeonggi-do 443-803, South Korea*

*faraon@caltech.edu

Abstract: An optical filter array consisting of vertical narrow-band Fabry-Pérot (FP) resonators formed by two highly reflective high contrast subwavelength grating mirrors is reported. The filters are designed to cover a wide range of operation wavelengths ($\Delta\lambda/\lambda = 5\%$) just by changing the in-plane grating parameters while the device thickness is maintained constant. Operation in the telecom band with transmission efficiencies greater than 40% and quality factors greater than 1,000 are measured experimentally for filters fabricated on the same substrate.

OCIS codes: (050.6624) Subwavelength structures; (050.2230) Fabry-Perot; (130.7408) Wavelength filtering devices.

References and links

1. B. Momeni, S. Yegnanarayanan, M. Soltani, A. A. Eftekhar, E. Shah Hosseini, and A. Adibi, "Silicon nanophotonic devices for integrated sensing," J. Nanophotonics **3**, 031001 (2009).
2. Z. Xia, A. A. Eftekhar, M. Soltani, B. Momeni, Q. Li, M. Chamanzar, S. Yegnanarayanan, and A. Adibi, "High resolution on-chip spectroscopy based on miniaturized microdonut resonators," Opt. Express **19**, 12356–12364 (2011).
3. B. B. C. Kyotoku, L. Chen, and M. Lipson, "Sub-nm resolution cavity enhanced microspectrometer," Opt. Express **18**, 102–107 (2010).
4. X. Gan, N. Pervez, I. Kymissis, F. Hatami, and D. Englund, "A high-resolution spectrometer based on a compact planar two dimensional photonic crystal cavity array," Appl. Phys. Lett. **100**, 231104 (2012).
5. S.-W. Wang, C. Xia, X. Chen, W. Lu, M. Li, H. Wang, W. Zheng, and T. Zhang, "Concept of a high-resolution miniature spectrometer using an integrated filter array," Opt. Lett. **32**, 632–634 (2007).
6. X. Wang, A. Albrecht, H. H. Mai, C. Woidt, T. Meinl, M. Hornung, M. Bartels, and H. Hillmer, "High resolution 3D NanoImprint technology: Template fabrication, application in Fabry-Perot-filter-array-based optical nanospectrometers," Microelectron. Eng. **110**, 44–51 (2013).
7. J. Xiao, F. Song, K. Han, and S.-W. Seo, "Fabrication of CMOS-compatible optical filter arrays using gray-scale lithography," J. Micromech. Microeng. **22**, 025006 (2012).
8. P. Lalanne, J. P. Hugonin, and P. Chavel, "Optical properties of deep lamellar Gratings: A coupled Bloch-mode insight," J. Lightwave Technol. **24**, 2442–2449 (2006).
9. C. F. Mateus, M. C. Huang, Y. Deng, A. R. Neureuther, and C. J. Chang-Hasnain, "Ultrabroadband mirror using low-index cladded subwavelength grating," IEEE Photonics Technol. Lett. **16**, 518–520 (2004).
10. D. Fattal, J. Li, Z. Peng, M. Fiorentino, and R. G. Beausoleil, "Flat dielectric grating reflectors with focusing abilities," Nat. Photonics **4**, 466–470 (2010).
11. C. Sciancalepore, B. B. Bakir, and S. Menezo, "III-V-on-Si photonic crystal vertical-cavity surface-emitting laser arrays for wavelength division multiplexing," IEEE Photon. Technol. Lett. **25**, 1111–1113 (2013).
12. A. Arbabi, Y. Horie, A. J. Ball, M. Bagheri, and A. Faraon, "Subwavelength-thick lenses with high numerical apertures and large efficiency based on high-contrast transmitarrays," Nat. Commun. **6**, 1–6 (2015).

#250298 Received 17 Sep 2015; revised 30 Oct 2015; accepted 2 Nov 2015; published 5 Nov 2015

13. D. L. Brundrett, E. N. Glytsis, and T. K. Gaylord, "Homogeneous Layer Models for High-Spatial-Frequency Dielectric Surface-Relief Gratings - Conical Diffraction and Antireflection Designs," Appl. Opt. **33**, 2695–2706 (1994).
14. V. Karagodsky, F. G. Sedgwick, and C. J. Chang-Hasnain, "Theoretical analysis of subwavelength high contrast grating reflectors," Opt. Express **18**, 16973–16988 (2010).
15. V. Karagodsky and C. J. Chang-Hasnain, "Physics of near-wavelength high contrast gratings," Opt. Express **20**, 10888–10895 (2012).
16. V. Liu and S. Fan, "S4: A free electromagnetic solver for layered periodic structures," Comput. Phys. Commun. **183**, 2233–2244 (2012).
17. S. Boutami, B. Benbakir, X. Letartre, J. L. Leclercq, P. Regreny, and P. Viktorovitch, "Ultimate vertical Fabry-Perot cavity based on single-layer photonic crystal mirrors," Opt. Express **15**, 12443–12449 (2007).
18. A. Ricciardi, S. Campopiano, A. Cusano, T. F. Krauss, and L. O'Faolain, "Broadband mirrors in the near-infrared based on subwavelength gratings in SOI," IEEE Photonics J. **2**, 696–702 (2010).
19. Z. Qiang, H. Yang, S. Chuwongin, D. Zhao, Z. Ma, and W. Zhou, "Design of Fano Broadband Reflectors on SOI," IEEE Photonics Technol. Lett. **22**, 1108–1110 (2010).
20. M. Shokooh-Saremi and R. Magnusson, "Properties of two-dimensional resonant reflectors with zero-contrast gratings," Opt. Lett. **39**, 6958–6961 (2014).
21. C. Sciancalepore, B. B. Bakir, X. Letartre, J.-M. Fedeli, N. Olivier, D. Bordel, C. Seassal, P. Rojo-Romeo, P. Regreny, and P. Viktorovitch, "Quasi-3D light confinement in double photonic crystal reflectors VCSELs for CMOS-compatible integration," J. Lightwave Technol. **29**, 2015–2024 (2011).
22. J. Li, D. Fattal, M. Fiorentino, and R. G. Beausoleil, "Strong optical confinement between nonperiodic flat dielectric gratings," Phys. Rev. Lett. **106**, 193901 (2011).

1. Introduction

The spectrometer is one of the most important instruments in the field of optics. Miniaturized spectrometers have been the subject of considerable recent interest due to their applications in a wide range of applications in sensing and various test and measurement equipment [1]. Several integrated optics approaches have been investigated, including ring resonator-based optical circuits [2], integrated diffraction grating [3], and photonic crystal cavity arrays [4]; however, low free-space to chip optical coupling efficiency reduces the sensitivity of these spectrometers. For free-space spectroscopy, one of the attractive designs consists of an array of on-chip narrowband wavelength optical filters directly placed on photodetector arrays [5]. In this design, a collimated incident light beam with a broadband spectrum of interest is filtered out

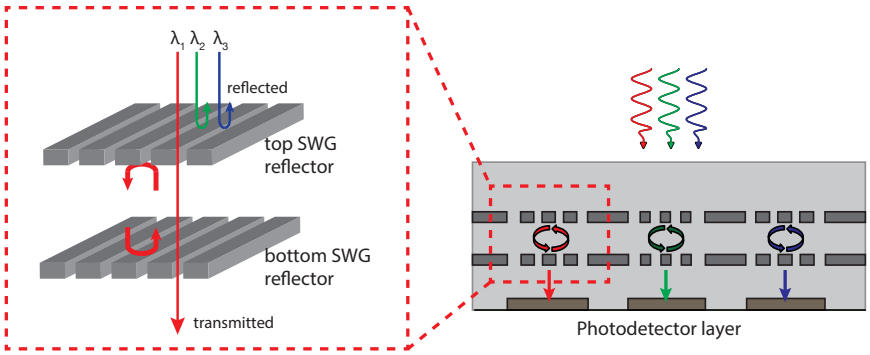

Fig. 1. Schematic illustration of narrowband wavelength filter array composed of vertical FP resonators realized using two-layers of SWG reflectors separated by a spacer layer. When broadband input light is illuminated, the spectrum is filtered out by the narrowband filters with different central wavelengths, and the optical powers detected by the underlying photodetector pixels are used to reconstruct the original spectral information.

#250298 Received 17 Sep 2015; revised 30 Oct 2015; accepted 2 Nov 2015; published 5 Nov 2015

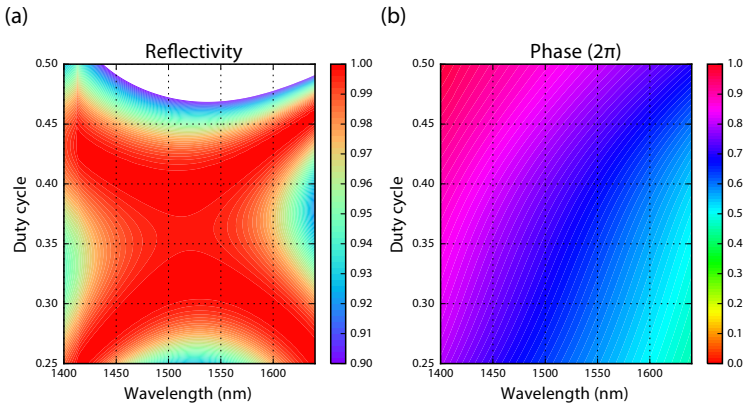

Fig. 2. (a) Simulated reflectivity contour map as a function of duty cycle of SWGs and wavelength, for the α-Si on SiO_2 1D SWGs with 900 nm period and SU-8 polymer cladding for the normally incident TE-polarized light (i.e. electric field parallel to the grating bars) and (b) the corresponding reflection phase contour map.

by the narrowband wavelength filters with different central wavelengths, and the corresponding underlying photodetectors are used to detect the optical power of the filtered spectra, allowing to reconstruct the spectral information for the incident light. Such a narrowband optical filter array is conventionally implemented by using FP resonators formed by two highly reflective distributed Bragg reflectors (DBRs) with spatially varied cavity length such that each of the resonators has a different resonance wavelength [6]. Grayscale lithographic technology enables the realization of cavities with spatially varied thickness in a controllable way as reported in [7]. However, such a high-end and expensive lithography is not readily available and hinders the realization of the narrowband optical filter array in mass production.

In this paper, we propose and demonstrate a method to design a set of narrowband filters that covers a wide range of wavelengths, based on a vertical FP resonators formed by two-layers of highly reflective subwavelength grating (SWG) reflectors [8, 9]. SWG reflectors not only provide broadband reflection spectra comparable to DBRs thus being regarded as the thin-layer alternatives of DBRs, but also, by changing the grating geometry, they allow for engineering the reflection phase while keeping their reflectivity very high [10]. In contrast to the conventional DBR-based vertical FP resonators, the resonance wavelengths of the SWG FP resonators can be controlled by adjusting in-plane geometries of the SWG reflectors [11]. Therefore, a set of narrowband filters can be easily fabricated using well-established top-down lithographic processes. As schematically shown in Fig. 1, each of the narrowband optical filters is made of two identical SWG reflectors separated by a distance on the order of a wavelength of interest, to satisfy the symmetric FP condition. Such symmetric FP resonators are critically coupled, have theoretical transmission of 100% at their resonance wavelength, and reflect back off-resonance portion of the incident light.

2. Design

To investigate the operation of the narrowband filters, we first designed a SWG reflector that operates in a wide wavelength range around the telecommunication band ($\lambda = 1550$ nm). The broadband SWG reflector design typically involves a subwavelength periodic structure made of a high-refractive index material surrounded by a low refractive index material. The subwavelength geometry of the grating suppresses higher order diffraction for normally incident light.

#250298 Received 17 Sep 2015; revised 30 Oct 2015; accepted 2 Nov 2015; published 5 Nov 2015

The high-index contrast system makes waveguide modes in the high index structure highly dispersive, opening up unique properties such as highly reflective [8–10] or transmissive [12] amplitudes in broadband, which cannot be explained by the traditional effective medium theory [13]. The details of the operating principle and design for the SWG reflector can be found in [14,15]. The SWG reflectors considered here are 1D gratings made of high-index amorphous silicon (α-Si) and embedded in low-index SU-8 polymer on a fused silica substrate. We used the rigorous coupled-wave analysis (RCWA) technique [16] to find the optimal SWG reflector designs. The basic reflectors designed for the normally incident TE-polarized light (i.e. electric field parallel to the grating bars) have a period of 900 nm and a grating thickness of 310 nm. Figure 2 shows the reflectivity and the associated reflection phase for the SWG reflectors as a function of the SWG duty cycle and the wavelength.

When two of such SWG reflectors are placed in parallel [17] and separated by a 1.23 μm-thick SU-8 spacer layer, a single FP resonance within the highly reflective stopband is observed. The SU-8 spacer layer thickness between the two SWG layers must be thicker than at least half of the wavelength such that evanescent field coupling between the two SWG layers is avoided. The low near-field coupling between the gratings reduces the sensitivity of the structure on the in-plane translational misalignment of the two gratings. The rotational misalignment of the two gratings should become more sensitive when 1D gratings are used, but can be tolerated using polarization-independent 2D SWG designs discussed later. Using the results for the SWG reflectors, the resonance wavelengths of the FP resonators were calculated while varying the in-plane grating parameters such as period and duty cycle, while keeping the grating thickness fixed. To ensure proper spectral filtering function, it is important to avoid the overlap of the FP resonance with other undesired resonances or the stopband edge of the SWG reflectors. Then, a set of optimum filter designs which provide a wide wavelength range of operation as well as narrowband transmission was identified. The simulated transmission spectra of these filters are plotted in Fig. 3(a). The simulations were performed using RCWA techniques. Filtering operation over a wide range of $\Delta\lambda = 70$ nm ($\Delta\lambda/\lambda = 5\%$) with moderately high quality factors larger than 1,000 can be achieved in the SU-8/Si/SiO_2 high index contrast system by introducing changes both in the duty cycles and periods of the SWG reflectors. The variation in the peak transmittance of the filters is caused by the different reflection amplitudes for the top and bottom SWG reflectors, which led to over- or under-coupling condition for some of the filters. The wavelength coverage can be further increased by using higher index contrast gratings such as air cladded silicon gratings which provide a broader SWG reflection stopband. Since the structure can be scaled with the wavelength, the proposed design is readily applicable to any wavelengths of interest provided a high-index contrast material combination with low loss is available. The 1D SWG reflector we use here shows large reflectivity only for the TE polarization and as a result, the narrowband filters work only for the TE-polarized light; however, polarization-insensitive filters can also be designed by replacing the 1D SWG reflectors with polarization-insensitive 2D SWG reflectors [18–20].

Simulated angular dependence of the transmission spectrum of one of the filters is presented in Fig. 3(b), showing that the resonance wavelength is shifted to a shorter wavelength for larger angles of incidence. The maximum transmittance is also decreased as the angle of incidence changes because the reflection amplitudes for the top and bottom SWG reflectors become more different as the angle of incidence changes. This behavior is unique, compared to the FP cavity using a pair of DBRs, as the reflection coefficient for SWG reflectors has more angular dependence than DBRs. From the angular response of the SWG reflectors, one can calculate cavity transmission spectra under Gaussian beam illumination: First, using the Fourier transform, the incident Gaussian beam is expanded in terms of plane waves propagating at different angles. Then, the amplitude of each of the transmitted plane waves is found using their amplitude in the

#250298 Received 17 Sep 2015; revised 30 Oct 2015; accepted 2 Nov 2015; published 5 Nov 2015

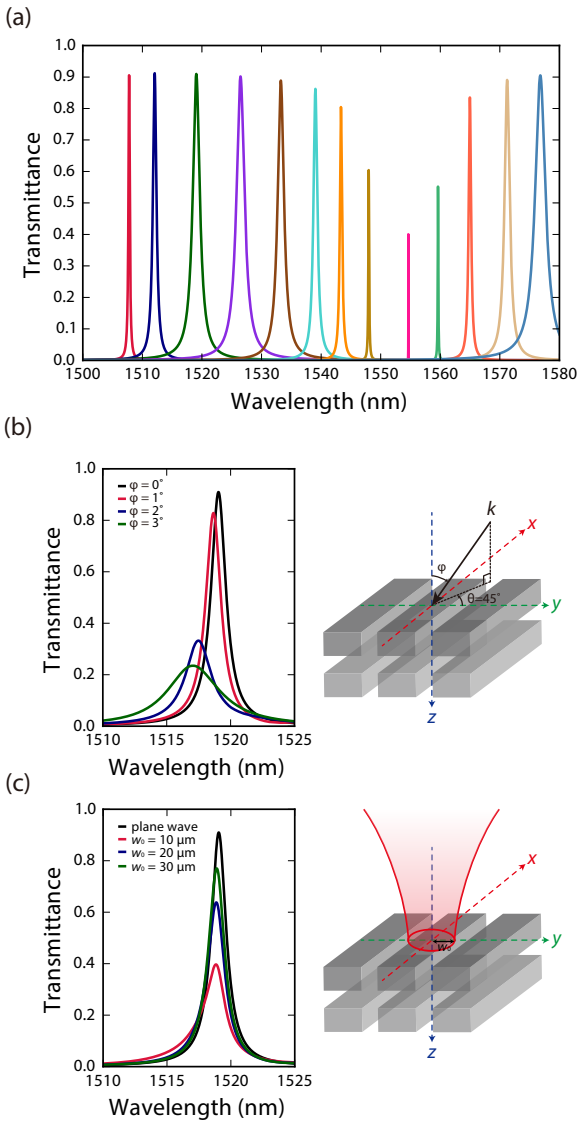

Fig. 3. (a) Simulated transmission spectra of a normally incident plane wave for a set of narrowband filters. (b) Angular dependence of the simulated transmission spectrum of one of the filters with an azimuthal angle of $\theta = 45°$ and various polar angles ϕ. (c) Simulated transmission spectra of one of the filters when illuminated with Gaussian beams with different beam waists w_0.

expansion and their corresponding transmission coefficient which is computed using RCWA. Finally, the transmitted beam is found by adding the contributions from all the plane waves (i.e. by an inverse Fourier transform). Figure 3(c) shows the simulated transmission spectra for normally incident Gaussian beams with different beam waists computed using this technique. It is assumed that the beam waist is at the same plane as the top SWG. As the beam waist gets smaller, the maximum transmittance is decreased because Gaussian beams with smaller beam waists have a larger plane wave angular spectrum and, as Fig. 3(b) indicates, the critical cou-

#250298 Received 17 Sep 2015; revised 30 Oct 2015; accepted 2 Nov 2015; published 5 Nov 2015

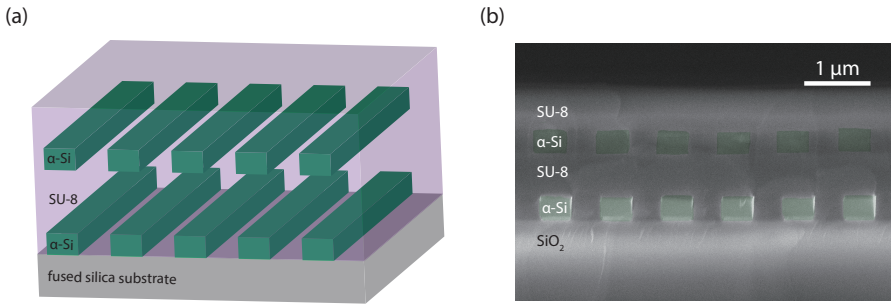

Fig. 4. (a) Schematic of a narrowband filter made of two-layers of SWG reflectors in the SU-8/α-Si/SiO_2 system. (b) Cross-sectional scanning electron microscope image of a fabricated narrowband filters.

pling condition is not met for plane waves with non-normal incidence angles. Thus, one can expect the maximum transmittance as well as a higher quality factor when the filters are tested using a collimated light rather than the focused light. Several approaches have been reported to achieve the lateral confinement by effective index confinement method [21] or reflector phase gradient approach [22], which could help to design the laterally confined resonator with better transmission efficiencies.

3. Method and results

3.1. Fabrication of narrowband filters

As a proof of concept, the narrowband filter array using the two-layers of SWG reflectors was fabricated on a fused silica substrate as illustrated in Fig. 4(a). First, an α-Si layer was deposited with a thickness of 310 nm by plasma-enhanced chemical vapor deposition (PECVD) method. The grating pattern was defined by electron beam lithography using a positive resist (ZEP-520A) followed by inductively coupled plasma reactive ion etching (ICP-RIE) process using SF_6/C_4F_8 mixed plasma chemistry for patterning the first α-Si layer. The patterned α-Si was planarized by spin-coating with SU-8 2002 followed by thermal reflow at 250°C, ending up with a 1.23 μm spacer layer. Subsequenctly, a second layer of PECVD-grown 310 nm-thick α-Si layer was deposited on top of the planar SU-8 layer. Then, another layer of the SWG pattern was aligned to the fist layer and etched using the same lithographic mask and etching processes. Finally, the whole structure was cladded with SU-8, and planarized by reflowing the SU-8 at 250°C. A typical cross-sectional image of the fabricated double layers of SWGs is shown in Fig. 4(b).

3.2. Characterization

The fabricated narrowband filter array was characterized by measuring the transmission spectra of the filters using a tunable laser and collecting the transmitted light from the filters on an InGaAs photodetector. Using an objective lens, the collimated and linearly TE-polarized beam from the laser was focused onto each filter from the normal direction. The beam diameter at focus was about 20 μm. The measured transmission spectra for a set of narrowband filters are shown in Fig. 5. The quality factors of the filters range from 1,100 to 3,000 (the linewidths range from 0.5 nm to 1.4 nm) and the maximum transmission ranges from 40% to 65%, as expected for a Gaussian probe beam (Refer to the simulation of the beam diameter dependence shown in Fig. 3(c)). Compared with the simulated transmission spectra under a plane wave

#250298 Received 17 Sep 2015; revised 30 Oct 2015; accepted 2 Nov 2015; published 5 Nov 2015

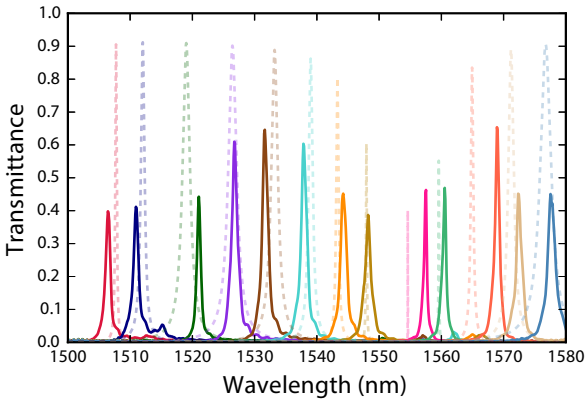

Fig. 5. The measured transmission spectra of a set of fabricated narrowband filters, where the grating duty cycle and period are controlled to obtain a sets of narrowband filters with different central wavelengths. The corresponding simulated transmission spectra for a normally incident plane wave illumination for the corresponding sets of narrowband filters are also shown in dotted lines.

illumination, the resonance wavelengths in the measured spectra have a good agreement with the numerical simulations and small discrepancies between the measured and simulated values are due to fabrication errors. Outside of the passband, the measured stopband transmittance was less than 1% within the wavelength range of interest, owing to the highly reflective properties of the designed SWGs. It is also worth to note that the system here is not limited by scattering or absorption loss. This was confirmed by checking that the sum of the transmitted and reflected power is constant around the resonances.

4. Conclusion

In conclusion, we proposed and experimentally demonstrated a narrowband filter array based on vertical FP resonators. The array of narrowband filters, each formed by two-layers of SWG reflectors, covers a wide range of wavelengths, owing to the broadband reflective designs of the SWGs, and the filtering wavelength can be controlled only by changing the in-plane SWG parameters. Highly compact on-chip spectrometers can be realized by integrating these filter arrays directly onto photodetector arrays.

Acknowledgment

This work was supported by Samsung Electronics and DARPA. Y.H. was also supported as part of the U.S. Department of Energy “Light-Material Interactions in Energy Conversion” Energy Frontier Research Center under grant DE-SC0001293 and a Japan Student Services Organization (JASSO) fellowship. The device nanofabrication was performed in the Kavli Nanoscience Institute at Caltech.